Supporting Information

Effect of Selenium Substitution on Intersystem Crossing in π-Conjugated Donor-Acceptor-Donor Chromophores: The LUMO Matters the Most

Rajendra Acharya, † *Seda Cekli,* † *Charles J. Zeman IV,* † *Rashid M. Altamimi,* ‡ *Kirk S. Schanze**,†

† Department of Chemistry and Center for Macromolecular Science and Engineering, University of Florida, Gainesville, Florida 32611-7200, United States.

‡ Petrochemicals Research Institute, King Abdulaziz City for Science and Technology, Riyadh, Kingdom of Saudi Arabia.

Corresponding Author

*kschanze@chem.ufl.edu

Experimental Methods:

Synthesis and Characterization: **Se-0 – Se-3** were synthesized following the literature or modified procedures, as outlined in detail below. All reactions (unless otherwise specified) were

carried out under dry argon. Reagents were purchased from Sigma-Aldrich, Alfa Aesar and Acros and used as received. The compounds were characterized by ^{1}H-NMR and ^{13}C-NMR and the data were correlated with literature data for the known compounds.

Photophysical Methods: Steady-state absorption spectra were recorded on a Shimadzu UV-1800 dual beam spectrophotometer. Steady-state fluorescence measurements were acquired on a Photon Technology International (PTI) spectrophotometer and are corrected for the spectral response of the instrument. Time-resolved fluorescence experiments were performed using a Picoquant FluoTime 100 time-correlated single photon counting (TCSPC) instrument. Data thus acquired were analyzed with FluoFit Software. Fluorescence quantum yields are reported relative to quinine sulfate standards and include ±10 % error. The sample solution had optical density of 0.03 - 0.07 and were excited at their λ_{max}. All the samples for absorption and emission experiments were prepared in THF solutions. Singlet oxygen quantum yield measurements were performed on a PTI Quantamaster near-IR spectrophotometer equipped with an InGaAs photodiode detector. Samples were prepared in deuterated chloroform ($CDCl_3$) and purged with oxygen for 10 min before the measurement. Singlet oxygen quantum yield values were reported relative to terthiophene (Φ_{Δ}=0.84) and include $\pm$15 % error.

The samples for nanosecond transient absorption (TA) spectroscopy were prepared in anhydrous THF with optical density 0.7 at the excitation wavelength and were degassed for 45 min. The TA system uses as an excitation source a Continuum Surelite series Nd:YAG laser (λ = 532 nm, 10 ns FWHM, 10 mJ/pulse) and a xenon flash lamp as a probe was used for measurement. TA signals were detected with a gated-intensified CCD mounted on a 0.18 M spectrograph (Princeton PiMax/Acton Pro 180). The optical density of the solutions was adjusted to ~0.7 at the excitation wavelength. The transient absorption (TA) spectrum was collected from

350 nm to 900 nm with a 60 ns initial camera delay and with different delay increments depending on the triplet lifetime of the molecule. Fifty averages were taken for each measurement.

Cyclic Voltammetry: Cyclic voltammetry (CV) study for the samples were performed using BAS CV-50W voltammetric analyzer. Samples were prepared in dry dichloromethane (CH_2Cl_2) in the presence of 0.1 M tetra-n-butylammonium hexafluorophosphate (TBAF) as supporting electrolyte. A platinum microdisk was used as a working electrode, platinum wire as an auxiliary electrode and silver wire as a pseudo-reference electrode. The sample concentrations were 1 mg/mL and cyclic voltammograms were recorded at a scan rate of 100mV/s under argon atmosphere. The HOMO and LUMO energy levels were calculated from the onset potentials using the following equations.[1,2]

$HOMO = -[(E_{ox,onset} - E_{1/2,\ Fc/Fc+}) + 5.1]$ eV

$LUMO = -[(E_{red,onset} - E_{1/2,\ Fc/Fc+}) + 5.1]$ eV

Where, $E_{ox,onset}$ and $E_{red,onset}$ are the observed onset oxidation and reduction potentials. $E_{1/2,\ Fc/Fc+}$ is half wave potential for ferrocene/ferrocenium redox couple vs Ag wire which was ~0.40 V in this study. The redox potential of Fc/Fc^+ is considered -5.1 eV relative to the vacuum level.

Computational Method: All calculations were performed with the Gaussian 09 suite of programs using DFT methods. The proposed conformations were optimized using the B3PW91 functional in conjunction with a 6-311G(2df,p) basis set[3]. Electronic spectra were calculated for the lowest energy conformation of each compound at the same level of theory using the TD-DFT program and the energy levels of the HOMO and LUMO were taken from these results. For MO composition analysis, output files for these conformations were prepared using the NAO Read option for the Population keyword. These output files were fed into the Multiwfn (v. 3.3.8)

software where percent contributions of individual atoms to specific molecular orbitals can be extracted. HOMO and LUMO compositions were taken from here. All calculations were done in vacuum.

Synthetic Schemes and Procedures:

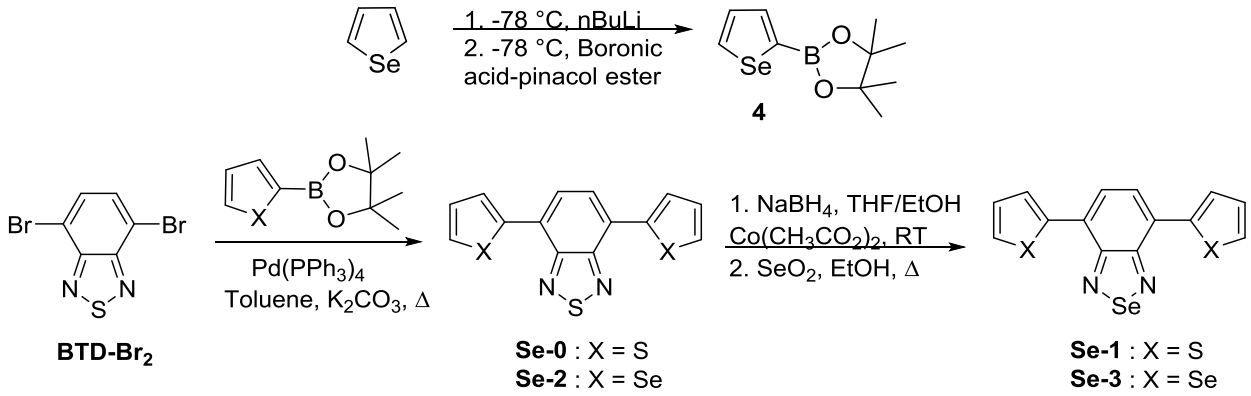

4,7-Di-thienyl-2,1,3-benzothiadiazole (Se-0): This compound was synthesized by following the literature procedure.[3,4] Orange red crystalline solid (0.61g, 58%). ^{1}HNMR (500 MHz, $CDCl_3$, ppm): δ 8.12 (d, *J* = 3.5 Hz, 2H), 7.88 (s, 2H,), 7.47(d, *J* = 4.8 Hz, 2H), 7.22(dd, *J* = 3.7 Hz, 2H). ^{13}CNMR (125 MHz, $CDCl_3$, ppm): δ 152.8, 139.5, 128.6, 127.8, 127.5, 126.6, 126.2.

Selenophene-2-boronic acid pinacol ester (**4**):[5] Selenophene (1.5 mL, 16.3 mmol) was dissolved in dry THF (20 mL) under argon and the solution was cooled down to -78˚C. At that moment, n-BuLi (8 mL, 2.5 M in Hexane) was added dropwise. The solution was stirred at that temperature for 1h. Again at -78˚C, 2-isopropoxy-4,4,5,5-tetramethyl-1,3,2-dioxyborolane (4 mL, 19.6 mmol) was added and stirred for 1h, then 12h at RT. Afterwards, ethylacetate (50 mL) was added and washed with water and $NaHCO_3$ solution. Organic layer was separated, dried over anhydrous Na_2SO_4 and evaporated under vacuum to obtain pale yellow oily liquid. The

crude product was separated on silica column using gradient of hexane: ethylacetate (95: 5 to 90: 10). Solvent was evaporated to obtain colorless crystalline solid (2.5 g, 60%). ^{1}HNMR (500 MHz, $CDCl_3$, ppm): δ 8.37 (d, *J* = 5.5 Hz, 1H, Ar), 7.97 (d, *J* = 3.5 Hz, 1H, Ar), 7.47 (t, *J* = 4.5 Hz, 1H, Ar), 1.36 (s, 12H, alkyl). Satellite peaks resulting from coupling with selenium are not included. ^{13}CNMR (125 MHz, $CDCl_3$, ppm): δ 139.7, 137.8, 131.1, 84.1, 82.9, 24.9.

4,7-Di-Selenyl-2,1,3-benzothiadiazole (Se-2):[6] In a 100 mL Schlenk flask, selenophene-2-boronic acid pinacol ester (1.5 g, 5.8 mmol), 4,7-dibromoselenadiazole (0.73 g, 2.5 mmol) and $Pd(PPh_3)_4$ (120 mg, 0.1 mmol) were added. It was then vacuum pumped and refilled with argon, repeated 3 times. Degassed toluene (30 mL) and degassed K_2CO_3 solution (2M, 15 mL) were added to the reaction mixture under argon. The reaction mixture was refluxed for 24 h. Then the reaction mixture was cooled to RT and organic layer was separated. Organic layer was washed with water, sodium bicarbonate solution and dried over anhydrous Na_2SO_4. The crude product obtained after evaporation of solvent was separated on silica column using a gradient of hexane: DCM (90: 10 to 75:25). Thus obtained orange solid was subsequently purified by recrystallization from DCM and methanol mixture to obtain flaky red crystalline solid (540 mg, 55%).^{1}HNMR (500 MHz, $CDCl_3$, ppm): δ 8.22 (dd, *J* = 6.2 and 5.6 Hz, 2H), 8.13 (d, *J* = 4 Hz, 2H), 7.83 (s, 2H), 7.44 (t, *J* = 4.7 Hz, 2H). Satellite peaks resulting from coupling with selenium are not included. ^{13}CNMR (125 MHz, $CDCl_3$, ppm): δ 152.6, 144.2, 133.6, 130.3, 128.4, 127.7, 125.2.

4,7-Di-thenyl-2,1,3-benzoselenadiazole (Se-1):[7] TBT (180 mg, 0.6 mmol) was dissolved in THF (50 mL) under argon and then ethanol (40 mL) was added. Reaction mixture was subsequently cooled to 0 ˚C and sodium borohydride (50 mg, 1.2 mmol) and cobalt acetate (40 mg, 0.2 mmol) were added to the reaction mixture and stirred. The orange colored solution

turned into colorless within less than 10 min. It was stirred further at RT for 30 min. Black particles formed in the solution was removed by filtration through a pad of neutral alumina on Hirsch funnel. Alumina layer was then washed with diethyl ether. Filtrate was collected and the solvent was evaporated. Off-white gummy solid thus obtained was used in next step without further purification.

The gummy solid was dissolved in ethanol (100 mL) and heated to reflux. Meantime selenium dioxide solution (10% in hot water, 5mL) was added dropwise. The reaction mixture immediately turned into bright red solution and was further refluxed for 2 h. Then the volume of the reaction mixture was reduced by using rotary evaporator and cooled down slowly to RT. Dark red crystals thus formed were collected by filtration and washed with water and methanol to obtain pure **Se-1** (165 mg, 80%).^{1}HNMR (500 MHz, $CDCl_3$, ppm): δ 8.0 (d, *J* = 3.7 Hz, 2H), 7.75 (s, 2H), 7.46 (d, *J* = 5 Hz, 2H), 7.19 (t, *J* = 4.5 Hz, 2H). ^{13}CNMR (125 MHz, $CDCl_3$, ppm): δ 158.4, 139.9, 127.9, 127.7, 127.6, 127.3, 126.2.

4,7-Di-selenyl-2,1,3-benzoselenadiazole (Se-3):[7] Same procedure followed as described above in **Se-1**. Cobalt acetate catalyzed $NaBH_4$ reduction of Se-2 and followed by oxidation using SeO_2 yielded pure **Se-3** as dark red crystalline solid (220 mg, 85%).^{1}HNMR (500 MHz, $CDCl_3$, ppm): δ 8.22 (d, *J* = 5.6 Hz, 2H), 8.09 (d, *J* = 3.8 Hz, 2H), 7.86 (s, 2H), 7.44 (dd, *J* = 3.9 Hz, 2H). Satellite peaks resulting from coupling with selenium are not included. ^{13}CNMR (125 MHz, $CDCl_3$, ppm): δ 158.2, 144.3, 134.5, 130.0, 129.3, 128.0, 125.2.

Optical band gap:

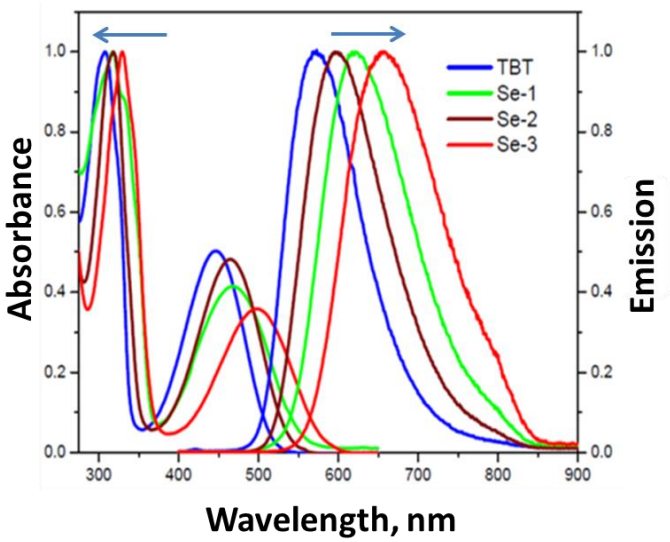

	Intersection Wavelength(nm)	Optical energy gap (eV)
Se-0	505	2.45
Se-1	540	2.29
Se-2	524	2.36
Se-3	565	2.19

Figure S1. Absorption and emission spectra showing intersection wavelengths. Optical energy gaps were calculated from those wavelengths.

Table S1. Photophysical measurements data of **Se-0 − 3**.

	Φ_{fl} [a]	τ [b] (ns)	Φ_{Δ} [c]	τ_T [d] (μs)	$E_g^{abs,e}$ (eV)	k_f [f] (10^7 s^{-1})	k_{isc} [g] (10^7 s^{-1})
Se-0	0.72	13.2	0.08	-	2.45	5.45	0.60
Se-1	0.37	15	0.29	0.68	2.29	2.46	1.93
Se-2	0.58	12.9	0.18	4.05	2.36	4.49	1.39
Se-3	0.26	17	0.48	0.48	2.19	1.53	2.82

[a] Fluorescence quantum yield, [b] fluorescence lifetime, [c] singlet oxygen quantum yields measured in $CDCl_3$. All other photo-physical measurements were performed in THF solution. [d] Triplet state lifetime, [e] Optical energy gap, [f] Fluorescence rate constant and [g] Intersystem crossing rate constant calculated by considering Φ_{Δ} as intersystem crossing quantum yield.

Rate constant calculation:

$k_f = \Phi_{fl} / \tau$ $\quad$ $k_{isc} = \Phi_{\Delta} / \tau$

Excited State Decay Kinetics:

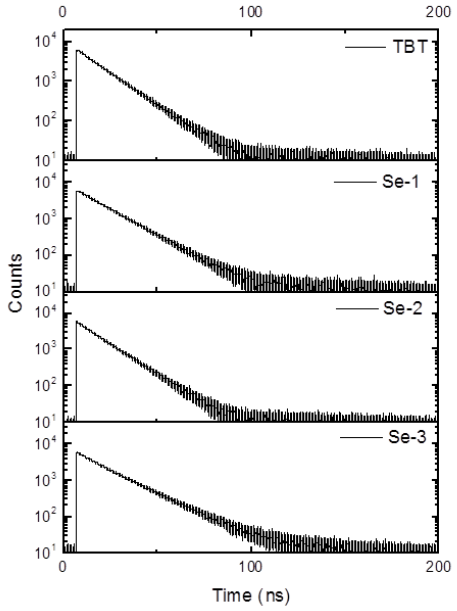

Figure S2. Fluorescence lifetime kinetic profile of **Se-0 – Se-3.**

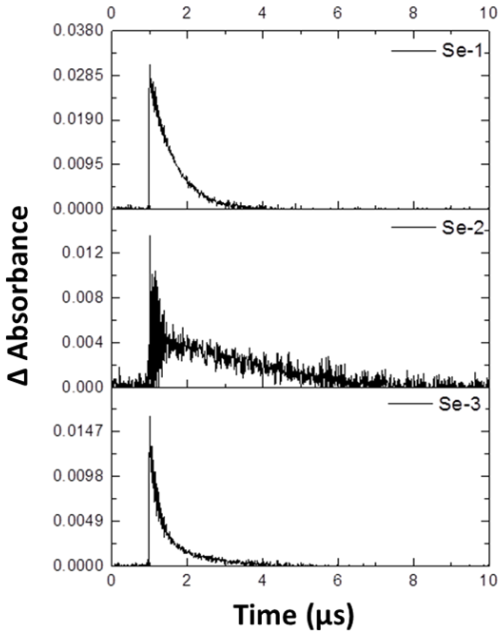

Figure S3. Triplet-triplet absorption decays of **Se-0- Se-3** monitored at 400 nm.

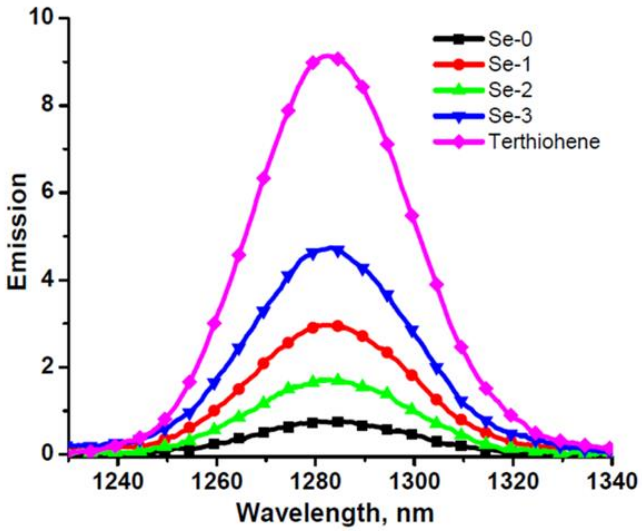

Figure S4. Phosphorescence of singlet oxygen observed with excitation of **Se-0** – **Se-3** and terthiophene at 326 nm in oxygenated $CDCl_3$ at room temperature. All the samples were purged with O_2 for 10 min.

Cyclic Voltammetry:

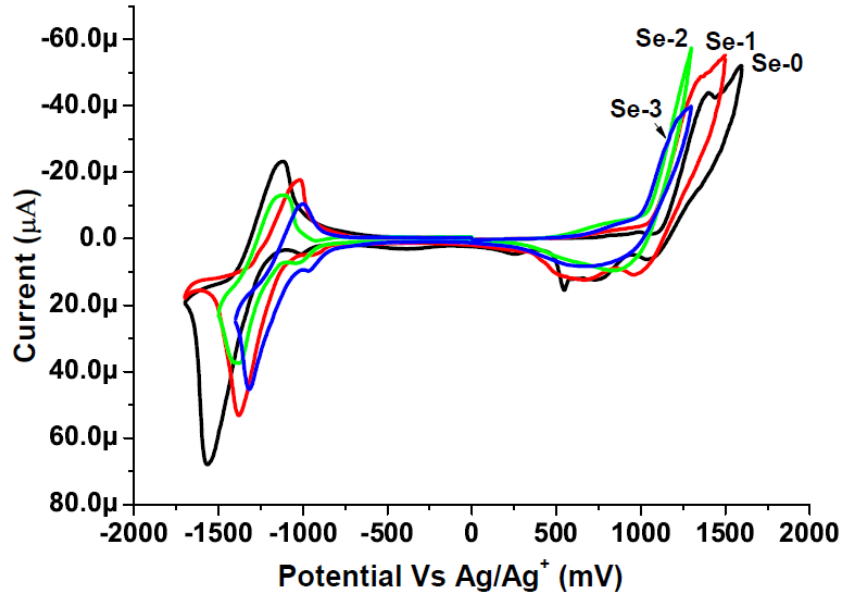

Figure S5. Cyclic voltammograms of **Se-0** – **Se-3** measured in CH_2Cl_2 (0.1M NBu_4PF_6 as supporting electrolyte). Platinum microdisk was used as a working electrode, platinum wire as an

auxiliary electrode and silver wire as a pseudo-reference electrode. Fc/Fc^+ redox couple was used as an internal reference.

Table S2. Electrochemical data and HOMO and LUMO energy levels of **Se-0 - Se-3**.

	$E_{ox,onset}$ (V)	$E_{red,onset}$ (V)	HOMO[a] (eV)	LUMO[a] (eV)	E_g[b] (eV)	HOMO[c] (eV)	LUMO[c] (eV)	E_g[d] (eV)
Se-0	1.12	- 1.21	- 5.52	- 3.19	2.33	- 5.66	- 2.87	2.79
Se-1	1.06	- 1.04	- 5.46	- 3.36	2.07	- 5.60	- 2.98	2.62
Se-2	1.04	- 1.12	- 5.44	- 3.28	2.16	- 5.58	- 2.96	2.62
Se-3	0.99	- 1.02	- 5.39	- 3.38	2.01	- 5.51	- 3.07	2.44

E_{ox} is first oxidation peak potential, $E_{1/2,red}$ is reduction half wave potential, $E_{ox,onset}$ and $E_{red,onset}$ are the observed onset oxidation and reduction peaks in forward sweep, [a] Electrochemical energy levels calculated from their corrected onset potentials, Fc/Fc^+ redox couple was used as a reference for correction, [b] Electrochemical energy gap, [c] Computational energy levels calculated the *B3PW91/6-311G(2df,p)* level, [d] Energy gap from computational data.

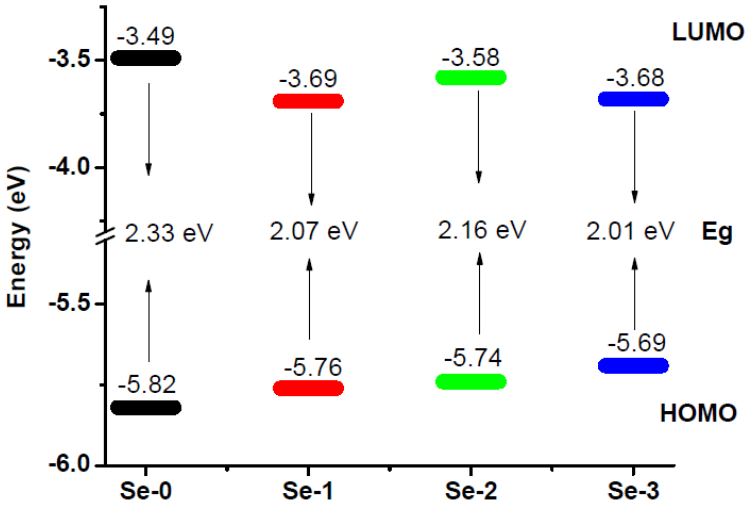

Figure S6. Electrochemical HOMO and LUMO energy and band gap of **Se-0− 3.**

DFT Calculations:

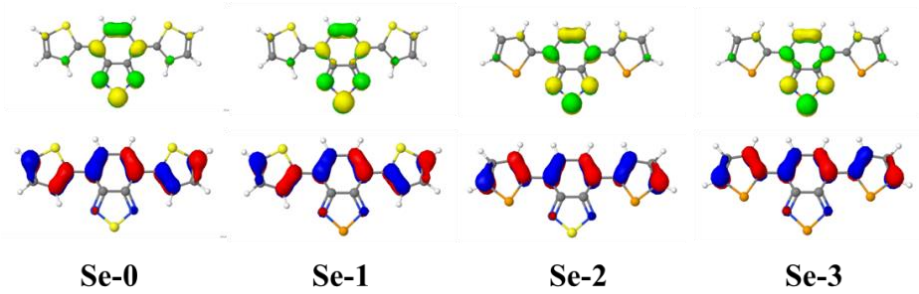

Figure S7**.** Illustrations of the HOMO (lower) and LUMO (upper) orbitals of **Se-0**−**3** calculated at the *B3PW91/6-311G(2df,p)* level.

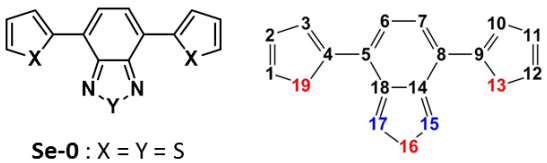

Se-0 : X = Y = S
Se-1 : X = S, Y = Se
Se-2 : X=Se, Y = S
Se-3 : X = Y = Se

Table S3 (a). HOMO composition analysis of **Se-0 − Se-3** showing percentage contribution of each atom.*

ATOM	**Se-0**	**Se-1**	**Se-2**	**Se-3**
1	10.837	10.582	11.54	11.492
2	2.979	2.945	2.631	2.471
3	7.193	7.124	7.98	8.111
4	7.874	7.607	7.986	7.756
5	9.923	10.151	9.425	9.573
6	6.042	6.36	5.593	5.895
7	6.042	6.36	5.593	5.895
8	9.923	10.151	9.425	9.573
9	7.874	7.607	7.986	7.756
10	7.193	7.124	7.98	8.111
11	2.979	2.945	2.631	2.471
12	10.837	10.582	11.54	11.492
13	1.377	1.453	0.999	0.896
14	1.026	0.796	1.136	0.91
15	2.396	2.637	2.375	2.56
16	0	0.001	0	0.001
17	2.396	2.647	2.375	2.56
18	1.026	0.796	1.136	0.91
19	1.377	1.453	0.999	0.896

Table S3 (b). LUMO composition analysis of **Se-0 − Se-3** showing percentage contribution of each atom.*

Atom	**Se-0**	**Se-1**	**Se-2**	**Se-3**
1	3.327	2.802	3.591	3.059
2	0.002	0.006	0	0.002
3	4.293	3.656	4.452	3.791
4	0.206	0.102	0.222	0.104

5	9.979	9.066	9.474	8.515
6	6.97	7.097	6.713	6.847
7	6.97	7.097	6.713	6.847
8	9.979	9.066	9.474	8.515
9	0.206	0.102	0.222	0.104
10	4.293	3.656	4.452	3.791
11	0.002	0.006	0	0.002
12	3.327	2.802	3.591	3.059
13	1.665	1.318	1.699	1.271
14	0.984	2.022	1.069	2.19
15	12.674	14.281	12.838	14.501
16	17.542	17.271	17.761	17.538
17	12.674	14.281	12.838	14.501
18	0.984	2.022	1.069	2.19
19	1.665	1.318	1.699	1.271

*Atom numbering scheme is shown in a figure above the table.

References for Supporting Information:

1. Thompson, B. C. Variable band gap poly (3, 4-alkylenedioxythiophene)-based polymers for photovoltaic and electrochromic applications. Ph.D. Dissertation, University of Florida, Gainesville FL, **2005**.
2. Cardona, C. M.; Li, W.; Kaifer, A. E.; Stockdale, D.; Bazan, G. C., Electrochemical considerations for determining absolute frontier orbital energy levels of conjugated polymers for solar cell applications. *Adv. Mater.* **2011,** *23*, 2367-2371.
3. Kitamura, C.; Tanaka, S.; Yamashita, Y., Design of narrow bandgap polymers. Syntheses and properties of monomers and polymers containing aromatic-donor and o-quinoid acceptor units. *Chem. Mater.* **1996,** *8*, 570-578.
4. Shin, W.; Jo, M. Y.; You, D. S.; Jeong, Y. S.; Yoon, D. Y.; Kang, J.-W.; Cho, J. H.; Lee, G. D.; Hong, S.-S.; Kim, J. H., Improvement of efficiency of polymer solar cell byincorporation of the planar shaped monomer in low band gap polymer. *Synth. Met.* **2012,** *162*, 768-774.
5. Haid, S.; Mishra, A.; Uhrich, C.; Pfeiffer, M.; Bauerle, P., Dicyanovinylene substituted selenophene thiophene co-oligomers for small molecule organic solar cells. *Chem. Mater.* **2011,** *23*, 4435-4444.
6. Alghamdi, A. A. B.; Watters, D. C.; Yi, H.; Al-Faifi, S.; Almeataq, M. S.; Coles, D.; Kingsley, J.; Lidzey, D. G.; Iraqi, A., Selenophene vs. thiophene in benzothiadiazole-based low energy gap donor–acceptor polymers forphotovoltaic applications. *J. Mater. Chem. A* **2013,** *1*, 5165-5171.
7. Pati, P. B.; Zade, S. S., Benzoselenadiazole Containing Donor−Acceptor−Donor Small Molecules: Nonbonding Interactions, Packing Patterns, and Optoelectronic Properties. *Cryst. Growth Des.* **2014,** *14*, 1695-1700.